Fast Nonlinear Magnetic Reconnection in Collisionless and Weakly Collisional Regimes

M Ottaviani, F Porcelli.

JET Joint Undertaking, Abingdon, Oxfordshire, OX14 3EA, UK.

Abstract

We analyse the nonlinear stage of magnetic reconnection in collisionless and weakly collisional regimes. The equilibria we consider are linearly unstable with the mode structure characterised by global convection cells. We find that the system exhibits a quasi-explosive time behaviour in the early nonlinear stage where the fluid displacement is smaller than the equilibrium scale length. The reconnection time is an order of magnitude shorter than the Sweet-Parker-Kadomtsev time for values of the skin depth and of the magnetic Reynolds number typical of core of large tokamaks. The reconnection process is accompanied by the formation of a current density sub-layer narrower than the skin depth. Mechanisms limiting the sublayer formation are also discussed.

Introduction

Laboratory plasmas close to thermonuclear conditions exhibit a variety of relaxation phenomena involving strong magnetic activity. The oldest known and best studied of these phenomena are sawtooth relaxations[1]. A common feature of these phenomena is the fact that they become more marked in the largest, hottest devices like JET. In JET, for example the ratio of the sawtooth period to the crash timescale exceeds three orders of magnitude. This is not unexpected on general grounds, since the crash time and the slow evolution should depend on different powers of the relevant Reynolds number (the magnetic Reynolds number).

Renewed interest in the crash problem was sparked by the observation[2] that at the high plasma temperatures of these experiments sawteeth can occur on a time scale shorter than the electron-ion collision time (see Fig. 1). Since the sawtooth phenomenon is associated with a reconnecting mode, the m=1 internal kink, this experimental findings have generated considerable interest in the problem of magnetic reconnection in collisionless regimes, where electron inertia is responsible for the decoupling of the plasma motion from that of the magnetic field.

Initially, the linear theory of m=1 kink-tearing modes was extended to the experimentally relevant regimes[3-6], leading to the conclusion that these modes can

remain virulent at low collisionality with an initial growth rate which compares favourably with that observed in the experiments. As usual, the validity of the linear theory is limited by the condition that the displacement of the magnetic axis does not exceed the width of the reconnecting layer, in practice the electron skin depth or the ion Larmor radius, whichever is larger. However the experiments show that the magnetic axis usually moves as fast as exponentially for a good fraction of the plasma size, well into the nonlinear stage.
So far, the nonlinear evolution has remained unclear. While Wesson's[7] modification of the Sweet-Parker-Kadomtsev scaling[8-10] has given an estimate of the collisionless reconnection time in good agreement with that observed experimentally, Drake&Kleva's numerical simulation[11] of the merging of two isolated flux bundles has led to the suggestion that the collisionless reconnection rate is greatly reduced as the nonlinear phase is entered, i.e. for magnetic island widths comparable with the plasma skin depth. This latter result would at least imply that the model studied cannot even qualitatively account for the experimental findings. This has induced some people to investigate the behaviour of more general models.
In this paper, it is our aim to clarify how reconnection proceeds in collisionless and weakly collisional plasmas. We will present the results of numerical and analytic investigation of a specific model, essentially the model studied in Ref.[12] where preliminary results were presented. The main conclusion will be that reconnection can proceed at a rate faster than the Sweet-Parker-Kadomtsev scaling well into the nonlinear regime, for a wide range of experimentally relevant conditions.

The model and its linear properties.

Our goal is to study the evolution of a reconnecting mode in the early nonlinear phase, defined by the condition $\delta_{linear} << \lambda << a$, where δ_{linear} is the width of the reconnection layer as given by linear theory, λ the displacement of the magnetic axis and a the macroscopic scale length (the plasma minor radius). In this regime the behaviour is expected to be universal, i.e. independent of the geometry. The model we consider is essentially an extension of reduced MHD on a slab, where the electron inertia terms, proportional to the square of the electron skin depth $d_e = c/\omega_{pe}$ is added in Ohm's law. For simplicity we neglect the Larmor radius effects, although these terms are formally of the same order as the skin depth terms. It is known from linear theory that Larmor radius effects are not sufficient to decouple the motion of the plasma from the magnetic field lines, but they can alter the dynamics when other reconnecting effects are present. We therefore consider the following equations:

$$\partial_t U + [\varphi, U] = [J, \psi] + \mu_i \nabla^2 U, \tag{1}$$

$$\partial_t F + [\varphi, F] = \eta \nabla^2 (\psi - \psi_o) - \mu_e \nabla^4 \psi, \tag{2}$$

where we use the notation $\partial_t \equiv \partial/\partial t$ and $[A,B] \equiv \mathbf{e}_z \cdot \nabla A \times \nabla B$, with $\boldsymbol{e}_z$ the unit vector along the z direction. $U = \nabla^2 \varphi$ is the fluid vorticity, φ is the stream function, $\mathbf{v} = \mathbf{e}_z \times \nabla \varphi$ is the fluid velocity, $J = -\nabla^2 \psi$ is the current density along z, ψ is the magnetic flux function ψ_o the equilibrium flux function, $F \equiv \psi + d^2 J$, with d the skin

depth. Moreover, we have explicitly added some dissipative effects proportional to the ion viscosity μ_i, the electrical resistivity η and the electron viscosity μ_e. Since the equations are normalized these dissipation coefficients must be interpreted as the inverse of Reynolds-like numbers. In the following, however, we will work with collisionless equations unless specified.
The co-ordinate z is ignorable, $\partial_z = 0$. The co-ordinates x and y vary in the intervals $x \in [-L_x, L_x]$ and $y \in [-L_y, L_y]$, with the slab aspect ratio $\varepsilon \equiv L_x/L_y < 1$. Periodic boundary conditions are imposed at the edge of these intervals. The magnetic field is $\mathbf{B} = B_o \mathbf{e_z} + \nabla\psi \times \mathbf{e_z}$, with B_o a constant value which we take to scale as $B_o \sim \varepsilon^{-1}|\nabla\psi|$ in order to mimic the magnetic field of a Tokamak. All quantities in Eqs. (1,2) are dimensionless, with L_x and $\tau_A = (4\pi\rho_m)^{1/2} L_x / B_y$ determining the length and time scale normalisation.

We consider an equilibrium specified by $L_x = \pi$, $\varphi_o = U_o = 0$, $J_o = \psi_o = \cos x$, and $F_o = (1+d^2)\psi_o$. This choice allows a completely analytic treatment of the linear problem. One finds that this equilibrium is tearing-unstable to linear perturbations of the type $(\varphi, \delta\psi) = \mathrm{Real}\{[\varphi_L(x), \delta\psi_L(x)] e^{\gamma t + iky}\}$, with $k = m\varepsilon$ and m an integer number, and with $\varphi_L(x)$ and $\delta\psi_L(x)$ respectively odd and even functions around the two equivalent reconnecting surfaces at $x = 0$ and at $x = \pm L_x$. In the limit $d << L_x$, the solution of the linearized system can be obtained analytically using asymptotic matching techniques. For $0 < k^2 \le 1$, the linearized mode structure in the *outer* region is $\delta\psi_L = \psi_\infty \cos[\kappa(|x| - \pi/2)]$ and $\varphi_L = (i\gamma/k \sin x)\delta\psi_L$, with ψ_∞ a constant and $\kappa \equiv (1-k^2)^{1/2}$. The logarithmic jump of $\delta\psi_L$ across the reconnecting layers is $\Delta' = 2\kappa \tan(\kappa\pi/2)$. In the choice of the slab aspect ratio we are moved by conflicting requirement. On the one hand, in analogy with the internal kink, we are interested the *large*-Δ' regime, defined by

$$\Delta' d \ge 1, \tag{3}$$

which can be satisfied for low values of m and $\varepsilon^2 << 1$ such that $\Delta' \sim (8/\pi k^2)$. In this regime, the structure of the stream function is macroscopic, with $\varphi_L \approx \varphi_\infty \,\mathrm{sign}\, x$, $\varphi_\infty \equiv (i\gamma/k)\psi_\infty$, everywhere except in narrow layers near the reconnecting surfaces. For $\Delta' d >> 1$, the eigenfunctions in the vicinity of the layer at $x=0$ take the form $\delta J_L \approx -\psi_\infty (2/\pi d^2)^{1/2} \exp(-x^2/2d^2)$ and $\varphi_L \approx \varphi_\infty \,\mathrm{erf}(x/2^{1/2} d)$, which match onto the outer solution for $|x| > d$. Thus, the current channel in the linear stage has a width $\delta_L \sim d$. The linear growth rate is $\gamma_L \approx kd$.
On the other hand we want just one mode (m=1) to become unstable. This sets a lower bound on the aspect ratio $\varepsilon = 1/2$, hence an upper bound on $\Delta' \approx 8.12$. Most of our studies were carried out with $d = 1/4$, thus satisfying the large Δ' condition as well as allowing a good scale separation ($d/2L_x = 0.04$).

General properties of the nonlinear collisionless model.

In this section we discuss some properties of Eqs. (1-2) in the inviscid (dissipationless) case.

We note that Ohm's law can be interpreted as a conservation law for the quantity F, which is recognised as the toroidal component of the canonical electron momentum, averaged over the distribution function. F is simply advected by the flow, which means that the value of F on a given fluid element is conserved. Related to this property is the existence of two families of invariants:

$$I_1 = \int dxdyf(F)$$

and

$$I_2 = \int dxdyUg(F)$$

where $f(F)$ and $g(F)$ are arbitrary functions. In addition the total energy is also conserved:

$$E = \tfrac{1}{2}\int dxdy[(\nabla\varphi)^2 + (\nabla\psi)^2 + d^2(\nabla^2\psi)^2]$$

We now show that the conservation of F generically implies the formation of singularities. Consider a hyperbolic stagnation point of the flow (X-point). Such points are for example the X- and the O-points of the isolines of ψ when the initial conditions for Eqs. (1-2) are the linear eigenfunctions. Assuming x to be the direction of the stable manifold one can approximate the equation of the fluid element as $dx/dt = -v_0(t)x/d$. Then the fluid elements converge exponentially to the X-point according to $x = x_0 e^{-\lambda/d}$, $\lambda(t) = \int_0^t v_0(\tau)d\tau$. If F has nonzero derivatives along x, these derivatives are exponentially amplified. Moreover, if F is analytic in the complex x-plane in a strip containing the x axis, the width of the strip will shrink exponentially. Thus the occurrence of a singularity at $t = +\infty$ is generic and does not occur only when the system evolves to a state of zero flow (a new equilibrium).

The formation of a singularity in F brings about a related current sheet around the X-point of the flux function, as discussed more in detail in the next sections.

We now present a more general heuristic argument as why singularities are expected in the evolution of fields satisfying equations like Eqs.(1-2) in the dissipationless case. Assume smooth initial conditions. The existence of derivatives of arbitrary order implies that the Fourier spectrum must decay at least exponentially at large wavenumbers. This means that although the spectrum will usually have a power law range, this would extend up to a maximum wavenumber, say k_M, where the exponential portion of the spectrum begins. Naturally k_M will change with time as the fields evolve. Three possibilities can in principle occur:

1) $k_M(t)$ stays bounded as $t \to +\infty$.

2) $k_M(t)$ grows indefinitely as $t \to +\infty$. The solution exists at all the times but the spectrum spreads as times goes on.

3) $k_M(t)$ becomes infinite at some finite time t_c. Then the field becomes singular and the solution ceases to exist.

The first option is not possible for *generic initial conditions*. Assume for the moment that $k_M(t)$ stays bounded. Then, upon truncating the equations to some wavenumber $k_U >> k_M$ one can replace the continuum system with a finite number of Fourier modes,

at the price of introducing an exponentially small error. However such a system will *in general* evolve into a power-law spectrum all the way to k_U (see Ref.[13]). This violates the assumption that the spectrum decays exponentially for $k > k_M$.
The third option is also unlikely to occur. Indeed a consequence of the existence of pointwise invariants like the vorticity has been used to show that the solution of the two-dimensional Euler equation remains C^∞ for all the times when the initial conditions are C^∞[14]. Although no proof is known for Eqs.(1-2) it is commonly thought that 2-d fluid equations possessing topologic invariants have the same properties. In Eqs.(1-2) the quantity F is such an invariant. Thus one concludes that a singularity will in general occur but only at $t = +\infty$.

Numerical Results: dissipationless case.

The numerical investigation of Eqs. (1,2) has been carried out with a pseudospectral code[15] which advances in time the Fourier representation of the field variables, truncated to 1024×64 (x,y) components. The initial conditions are chosen to approximate closely the linear eigenfunctions of the unstable model with small amplitudes. The spatial symmetries of the initial conditions, namely reflection symmetries with respect to the reconnection line and with respect to the four points $x = \pm L_x/2$, $y = \pm L_y/2$ are preserved during the nonlinear evolution.
Fig. 2 shows sections of $\delta\psi \equiv \psi - \psi_o$, $v_x = -\partial\varphi / \partial y$, J and F across the X-point ($y = 0$) at various times. Initially the systems evolves linearly until $t \sim 80$, when the magnetic island reaches a width of order d. The linear layer width $\sim d$ is visible from these graphs. For $t > 80$, the width of the profile of v_x, $\delta_\varphi \equiv (v_x)_{x=L_x/2} / (\partial_x v_x)_{x=0}$, as well as that of $\delta\psi$, remain of the order of the skin depth (Figs. 2a,b). By contrast, the current density profile (Fig. 2c) develops a sub-layer whose width around the X-point, $\delta_J \equiv \left(\partial_x^2 \delta J / \delta J\right)^{-1/2} < d$, keeps shrinking with time (see also Fig. 3d). Here, $\delta J \equiv J - J_o$.
This sub-layer is also visible in the profile of F across the X-point (Fig. 2d). The contraction of this sub-layer is extremely rapid in time, as shown by the graph of $\partial^2 F / \partial x^2$ versus y for $x = 0$ and several times in Fig. 3b. At $t \approx 125$, it has become so narrow that it can no longer be resolved by our truncated Fourier expansion, and so the simulation is stopped. Also shown in Fig. 3a and 3c are the profiles of $\delta\psi$ and of $v_y = \partial\varphi/\partial x$ along the reconnection line ($x = 0$) at various times, from which it is clear that only a limited number of Fourier harmonics along y are involved in the early non-linear evolution. Contour plots of φ, ψ, J and F are shown in Fig. 4. Note that the convection cells retain approximately their linear shape well into the nonlinear phase (Fig. 4a). Also note the development of a current sheet around the reconnection line (Fig. 4c) and the preservation of the topology of the isolines of F (Fig. 4d). Finally, Fig. 5 summarises the time behaviour. It is remarkable that the mode growth remains very rapid throughout the simulation. Indeed, the growth of φ, as well as that of $\delta\psi$ and δJ at the X-points, accelerate in the early nonlinear phase, which is symptomatic of an explosive behaviour. However, the mode growth slows down when w approaches L_x.

Analytic Approach.

The conservation of F allows the formal integration of the collisionless Ohm's law (2):

$$F(x,y,t) = F_o[x_o(x,y,t)] = (1+d^2)\cos[x_o(x,y,t)] \ , \tag{4}$$

where $x_o(x,\ y,\ t) = x - \xi(x,\ y,\ t)$ is the initial position of a fluid element situated at (x,y) at time t and ξ is the displacement along the x direction defined by the equation $d\xi/dt = \mathrm{v}_x$, $\xi(t=-\infty) = 0$. In order to proceed, we note that the numerical results suggest that the spatial structure of the stream function does not vary significantly with time throughout the linear and early nonlinear phases. This motivates the ansatz:

$$\varphi(x,\ y,\ t) = \mathrm{v}_o(t)g(x)h(y) + u(x,y,t) \ , \tag{5}$$

where $h(y) \sim k^{-1}\sin(ky)$, $g(x) \sim \varphi_L(x)/\varphi_\infty$ contains the linear scale length d and $u(x,y,t)$ develops the rapid scale length $\delta(t) \sim \delta_J$ observed in the numerical simulation. We assume $u << \mathrm{v}_o$ and $\partial_x u \sim \mathrm{v}_o \partial_x g$, which is consistent with the near constancy in time of the width of v_x across the reconnecting layer (Fig. 3d), as well as that of the ratio $\mathrm{v}_y\left(0, L_y/2, t\right)/\mathrm{v}_x\left(-L_x/2, 0, t\right)$ (Fig. 5). This assumption allows a parametrization of the system of Eqs. (1,2) in terms of the displacement $\lambda(t) = \int_0^t \mathrm{v}_o(\tau)d\tau$.

By integrating the equation of the fluid element along the line $y = 0$ (across the X-point), $dx/dt = \mathrm{v}_x$, and neglecting a small contribution from $u(x,y,t)$, one gets

$$-\int_{x_o}^{x} dx'/g(x') = \int_{-\infty}^{t} \mathrm{v}_o(t')dt' \equiv \lambda(t). \tag{6}$$

This equation can be inverted for a typical shape of the function $g(x)$. In the large Δ' regime, this function can be approximated as $g(x) = x/d$ for $|x| < d$ and $g(x) = \pm 1$ for $|x| > d$. This is equivalent to the statement that convective cells remain large throughout the early nonlinear stage without developing small scales (to the leading order). Inverting Eq. (6) one gets the dominant contribution to the function $x_o(x,\ y,\ t)$ in three characteristic spatial ranges bounded by the linear scale d and by the nonlinear microscale $\delta(t) \equiv d\exp[-\lambda(t)/d]$:

$$x_o \sim x(d/\delta) \qquad \text{for } |x| < \delta \tag{7a}$$

$$x_o \sim d\ln(e|x|/\delta)\mathrm{sign}(x) \qquad \text{for } d > |x| > \delta \tag{7b}$$

$$x_o \sim \lambda\,\mathrm{sign}(x) + x \qquad \text{for } |x| > d \tag{7c}$$

Analogous relations are obtained along the $ky = \pi$ line, crossing the O-point, by swapping x and x_o. A sketch of the dependence of x_o on x is presented in Fig. 6. Thus we see that near the X-point along the x direction, $F(x_o)$ (and hence J) varies over a distance $\delta(t)$ which becomes exponentially small in the ratio λ/d. Conversely, around the O-point $F(x_o)$ flattens over a distance $|x| \sim \lambda$ from the O-point. We stress again that the formation of a sub-layer is the combined result of the conservation of F on each fluid element and the flow pattern around the X-point (O-point), which acts to increase (decrease) the local curvature of the F profile (Fig. 2d).

The flux function can be expressed in terms of F by means of the proper Green's function. Here we neglect the derivatives along y, which is justified in the large Δ' limit. Moreover we replace the Green's function defined in the box with the one defined in the plane. This is a valid approximation in the range of interest $x < \lambda << L_x$:

$$\psi(x,y,t) \approx \tfrac{1}{2}\int_{-\infty}^{\infty} e^{-|\hat{x}-\hat{x}'|} F(\hat{x}',y,t)\,d\hat{x}', \tag{8}$$

where $\hat{x} \equiv x/d$. One can notice that ψ has an integral structure such that any fine scale variation of F is smoothed out over a distance $\sim d$. Asymptotic evaluation of the deviation from the equilibrium $\delta\psi$ at the X- and O-points gives

$$\delta\psi_X \sim -\tfrac{1}{2}\lambda^2(t), \quad \delta\psi_O = \mathcal{O}(d^2). \tag{9}$$

The conservation of F implies $\delta F = 0$ on the reconnection line, so $\delta J = -\delta\psi/d^2$. Thus we have demonstrated that an asymmetry develops in the values of $\delta\psi$ and of J between the X- and O-points. The spike of the current density at the X-point has an amplitude $\delta J_X \sim 0.5(\lambda/d)^2$.

It is useful to analyse the behaviour away from the X-point obtained from Eq. (8). The leading contributions to $\delta\psi$ are:

$$\delta\psi = -\tfrac{1}{2}\lambda^2 + \mathcal{O}(\lambda d) \qquad \text{for } x < d \tag{10a}$$

$$\delta\psi = -\tfrac{1}{2}\lambda^2 - \lambda x + \mathcal{O}(d^2) \qquad \text{for } d < x << L_x \tag{10b}$$

There are however subdominant logarithmic corrections to Eq. (10a) which turn out important when computing the current. This can be done directly from the expression $\delta J = (\delta F - \delta\psi)/d^2$:

$$\delta J = -\tfrac{1}{2}\lambda^2/d^2 \qquad \text{for } x < \delta \tag{11a}$$

$$\delta J \approx -(\lambda/d)\ln(x/d) - \tfrac{1}{2}[1+\ln(x/d)]^2 + \mathcal{O}(\lambda/d) \qquad \text{for } \delta < x < d \tag{11b}$$

$$\delta J = \mathcal{O}(\lambda/d)\exp(-x/d) \approx 0 \qquad \text{for } x > d \tag{11c}$$

Let us now integrate the vorticity equation (1) over the quadrant $S{:}\left[0 \le x \le L_x, 0 \le y \le L_y\right]$. Using Stokes theorem, we obtain

$$\partial_t \int_C \mathbf{v}\cdot d\mathbf{l} = \oint_C \omega d\varphi + \oint_C J d\psi = \oint_C J d\psi. \tag{12}$$

where C is the boundary of S, i.e. the quadrangle XO'X'O which connects the critical points of the two symmetric islands. We have use the fact that $d\varphi = 0$ on C. By exploiting the symmetry with respect to $(L_x/2, L_y/2)$ one realises that it is enough to integrate along the lines OX and XO'. As a rule the integrals along XO' gives only a subdominant contributions in the large Δ' limit.

The l.h.s. of Eq. (12) is dominated by the integral of v_y (the integral of v_x contributes to order $\mathcal{O}(\varepsilon kd)$). Using the ansatz (5), and neglecting corrections contributed by $\partial_y^2\varphi$, we find

$$\partial_t \int_C \mathbf{v}\cdot d\mathbf{l} \approx -\left(2c_0c_1/k^2d\right)d^2\lambda/dt^2\,, \tag{13}$$

where $c_0 = d\,(dg/dx)_{x=0} = \mathcal{O}(1)$ and $c_1(t) = 1+(d/c_0 v_o)(\partial_x u)_X$ is a factor of order unity, which depends weakly on time (e.g. $1 \le c_1 \le 1.4$ in Fig. 3d).
The r.h.s. of Eq. (12) can be written as

$$\oint_C J d\psi = -\int_0^{L_y} dy\left(J\,\partial_y\psi\right)_{x=0} - \int_0^{L_x} dx\left[(\partial_y^2\psi)(\,\partial_x\psi)\right]_{y=0}.$$

The first integral at the right hand side can be evaluated exactly:

$$-\int_0^{L_y} dy\left(J\,\partial_y\psi\right)_{x=0} = \delta\psi_X - \delta\psi_O - \left(\delta\psi_X^2 - \delta\psi_O^2\right)/2d^2\,. \tag{14}$$

The second integral is bounded to $\mathcal{O}(k^2\lambda)$, which is subdominant both in the linear and in the nonlinear phase.

Using an interpolation formula between the linear and early nonlinear limits of the r.h.s. of (14), we obtain an equation for the evolution of $\hat{\lambda}(t) \equiv \lambda(t)/d$:

$$d^2\hat{\lambda}/d\hat{t}^2 \approx \hat{\lambda} + c_2\hat{\lambda}^4 \tag{15}$$

where $\hat{t} \equiv \gamma_L t$ and $c_2 \approx 1/16c_0c_1$ can be taken constant. The solution is $\hat{\lambda}(\hat{t}) = \left[(1-\alpha)/\left(1-\alpha\, e^{3\hat{t}}\right)\right]^{2/3} e^{\hat{t}}$, where $\alpha = \beta - \left(\beta^2-1\right)^{1/2}$, $\beta = 1+5/c_2$, and we have chosen the time origin so that $\hat{\lambda}(0) \equiv 1$. Thus, once the early nonlinear regime is entered, $\lambda(t)$ accelerates and reaches a macroscopic size over a fraction $\sim \ln\left(\alpha^{-1/3}\right)$ of the linear growth time. This acceleration is clearly visible in Fig. 5. Detailed comparison of the prediction of Eq. (15) and the result of the numerical experiment is however made difficult by the resolution which limits $\hat{\lambda}$ to $\hat{\lambda} = \ln(d/\delta_{\min}) \approx 3.7$.
This explosive growth will eventually turn into a slower growth as λ approaches the macroscopic scale length. It is interesting to ask whether there is bound on the growth of λ. Within this model there is an overall bound to the maximum attainable velocity set by the energy conservation law. This means that, asymptotically, λ cannot grow faster than linearly in time. In this range λ would cease to be the displacement as it would grow bigger than the macroscopic length. However other physical limitations to the displacement growth would intervene much earlier. Some of them will be discussed later.

Numerical results with dissipation.

We now discuss how a small amount of dissipation modifies the previous phenomenology. We have not investigated the case $\mu_i \neq 0$ so we will only consider $\mu_e \neq 0$ and/or $\eta \neq 0$ in this section. The goal is to investigate how the spike evolution is affected, so one is usually interested in the behaviour of the model (1-2) with finite values of d but sufficiently small dissipation coefficients. In particular the

It is interesting, however, to compare the previous collisionless results with a pure resistive case, $d=0$ but $\eta \neq 0$. To this end, we have initialised the system with the same eigenfunctions. It is possible to show that linear theory is unaffected by a change of the pair of values of (η,d) if the growth rate and the quantity $\eta+d^2\gamma$ are held constant. This corresponds to $\eta = 3.\times 10^{-3}$ when $d=0$. The nonlinear stage is however completely different as seen from Fig. 7. In particular the development of the current sheet proceeds in a much slower fashion than in the collisionless case. In general we do not find any particular reason why the system should not follow the Sweet-Parker behaviour. It must be pointed out, however, that a detailed analysis would require smaller values of the resistivity which, in turn, would violate the large Δ' condition for our system.

We now investigate whether the resistivity can act as spike-limiting mechanism. By inspecting Ohm's law (2) using the expressions for the flux function and for the current given by Eqs. (10-11), one can see that the resistive term in the spike region is bounded to $\mathcal{O}(\eta\lambda^2/d^2)$ which is smaller than the l.h.s. of Eq. (2) (which is $\mathcal{O}(\lambda d\lambda/dt) \geq \mathcal{O}(\gamma_{linear}\lambda^2)$) for small values of η. In other words the resistivity term is a regular perturbation (the order of the differential operator is too low) and it is not effective as a small scale cut-off. This situation persists as long as $\eta < \gamma_{linear} d^2$. This also the condition to neglect the resistivity in the linear theory.

On the other hand, the electron viscosity term is $\mathcal{O}[\mu_e(\lambda/d)(1/x^2)]$ and can balance the leading collisionless terms at a sufficiently close distance from the X-point. Thus the electron viscosity is an efficient spike-limiting mechanism. It should be remarked that one does not necessarily thinks of a true (collisional) viscosity at this point: any process acting as a current hyperdiffusivity would be a potential candidate.

This ideas have been confirmed by running simulations with $\mu_e = 0$ and η up to $\eta = 1.5\times 10^{-3}$ and $\eta = 0$ with μ_e in the range $4.\times 10^{-7} \leq \mu_e \leq 6.4\times 10^{-6}$.

We have not run simulations with $d < \eta^{1/3}$ because it is not possible to use small enough values of the resistivity without violating the large Δ' condition. In the rest of this section we present our conjectures about the likely behaviour in this regime.

When $d < \eta^{1/3}$ the electron inertia terms are negligible in the linear phase and the displacement grows with $\gamma_{linear} \approx \eta^{1/3}$ until the displacement is of order of the width of the linear layer $\lambda \approx \delta_{linear} \approx \eta^{1/3}$. In the nonlinear stage the behaviour will initially follow the Sweet-Parker scenario with the layer width shrinking as $\delta_{nonlinear} \approx (\eta/\lambda)^{1/2}$ while the displacement grows as a power law $\lambda \approx \eta t^2$. If $d < \eta^{1/2}$ (*strong collisionality*) nothing can stop the displacement from reaching the macroscopic size $\lambda \approx 1$ when $\delta_{nonlinear} \approx (\eta)^{1/2}$. In this case the reconnection proceeds in a purely resistive fashion and needs the characteristic Sweet-Parker-Kadomtsev time $\tau_{KSP} \approx \eta^{-1/2} \approx (\tau_{Alfven}\tau_{Resistive})^{1/2}$ to be completed. When however the skin depth falls in the intermediate range $\eta^{1/2} < d < \eta^{1/3}$ (*moderate collisionality*) a new regime occurs[16]. In this case the inertia terms become important when $\delta_{nonlinear} \approx d$. This occurs at some value of the displacement $\lambda^* \approx \eta/d^2$ after a time $t^* \approx d^{-1}$. Afterwards we expect that the reconnection will proceed essentially in a collisionless fashion until $\lambda \approx 1$. The reconnection time is therefore controlled by the electron inertia, $\tau_{rec} \approx d^{-1} << \tau_{KSP}$, throughout the collisionless and the moderate collisionality regimes. Of experimental interest is the borderline between these regimes, which is typical of large tokamak

sawteeth: here the reconnection time turns out at least an order of magnitude shorter than the Sweet-Parker-Kadomtsev time: $\tau_{rec} / \tau_{KSP} \approx \eta^{-1/6} > 10$.

Discussion and conclusions

The previous results have been obtained analysing the simplest possible fluid model which exhibits collisionless reconnection. The key effect is played by the electron inertia, therefore we have used a version of the generalised Ohm's law which includes just the skin depth terms, neglecting the terms associated with the parallel gradient of the electron pressure. This approximation is valid as long as the skin depth is bigger than the ion sound Larmor radius, $\rho_s < d_e$. When this occurs one can show that the fluid approximation is valid.
The linear theory in the opposite regime[3-6] is complicated by the fact that, although $\rho_s > d_e$, one cannot neglect the inertia terms otherwise reconnection does not take place. The existence of two distinct scale lengths brings two nested singular layers into the problem $\delta_{in} \approx d(\rho_s / d)^{-1/3}$ and $\delta_{out} \approx \rho_s$. The main result is that the growth rate is enhanced by a factor $(\rho_s / d_e)^{2/3}$: $\gamma \approx \gamma_A d_e (\rho_s / d_e)^{2/3}$. In this regime it was shown that the linear theory can be consistently developed within the fluid approximation using the isothermal equation of state. This equation of state turns out valid at any distance from the rational surface bigger than the inner layer width: $x > \delta_{in}$. This is enough to carry out the asymptotic matching at the inner layer. Moreover the condition that resonance effects do not occur, $\omega^* / \omega << 1$, is also fulfilled provided that β is sufficiently small and the density gradient sufficiently flat. When this occurs, the kinetic treatment is not necessary to develop the linear theory
The validity of fluid theory in the nonlinear regime when $\rho_s > d_e$ is more delicate. The point is that as the current spike develops the electron velocity distribution becomes distorted, the current being carried by energetic electrons. At the same time the nonlinear scalelength associated with the spike becomes rapidly smaller than the inner layer width $\delta_{nonlinear} < \delta_{in}$. Thus no equation of state can be used uniformly in this regime, and a kinetic treatment, even in the absence of resonances seems unavoidable.

The width of the current spike predicted by our model becomes rapidly small. When the displacement has become few times the skin depth, the width of the spike has decreased to values comparable to the Debye length or to the electron Larmor radius. It is therefore relevant to ask what are the physical mechanisms which could slow down the process of the current spike formation. *More importantly, to understand the experimental findings, is to verify whether the fast growth of the displacement can be sustained even in the presence of spike cut-off mechanisms.*
As far as the actual cut-off mechanisms, we have discussed the possible role of dissipation in the previous section. Other possibilities to be explored include instabilities of the current sheet. Note that our calculation assumes a well defined parity in the initial conditions. When this constrained is relaxed, secondary instabilities of different parity can occur. Another possible current instability (not treatable within our model) is two-stream instability associated with the distortion of the electron velocity distribution function[17]. Finally we note that stochasticity associated with three-dimensional geometry can also be effective, especially since fast electron are generated.

In conclusion, collisionless reconnection in regimes where the instability parameter Δ' is large and global convection cells develop does not follow the standard Sweet-Parker scenario. In these regimes, the reconnection rate accelerates nonlinearly. The physical mechanisms for this acceleration has been identified in the electromagnetic torque $\oint_C \mathbf{J}\times\mathbf{B}\cdot\mathbf{dl} = \oint_C J d\psi$ associated with the X-point/O-point asymmetry.

The simple model we have investigated has a number of limitations. However, from what has emerged from our analysis, we are led to believe that the occurrence of a rapid nonlinear stage, when the system evolves faster than Sweet-Parker-Kadomtsev timescale, is a fairly general phenomenon in weakly collisional systems characterised by large values of the Δ' parameter. We hope that present analysis will open the possibility to understand the rapidity of relaxation processes observed in low collisionality plasmas.

The authors acknowledge stimulating discussions with F. Pegoraro, F. Waelbroeck, J. Wesson and L. Zakharov.

References

[1] S. von Goeler, W. Stodiek and N. Sauthoff, Phys. Rev. Lett. **33**, 1201 (1974).
[2] A.W.Edwards et al, Phys. Rev. Lett. **57**, 210 (1986).
[3] F.Porcelli, Phys. Rev. Lett. **66**, 425 (1991).
[4] H.L.Berk, S.M.Mahajan and Y.Z.Zhang, Phys.Fluids **B3**, 351 (1991).
[5] B.Coppi and P.Detragiache, Phys. Lett. **A168**, 59 (1992).
[6] L.E.Zakharov and B.Rogers, Phys. Fluids **B4**, 3285 (1992).
[7] J.Wesson, Nuclear Fusion **30**, 2545 (1990).
[8] P.A.Sweet, in *Electromagnetic Phenomena in Cosmic Physics*, ed. by B.Lehnert (Cambridge University Press, 1958), p. 123.
[9] E.N.Parker, J. Geophys. Research **62**, 509 (1957).
[10] B.B.Kadomtsev, Fiz. Plasmy **1**, 710 (1975) [Sov. J. Plasma Phys. **1**, 389 (1975)]
[11] J.F.Drake and R.G.Kleva, Phys. Rev. Lett. **66**, 1458 (1991).
[12] M. Ottaviani and F. Porcelli, Phys. Rev. Lett. **71**, 3802 (1993).
[13] R. Kraichnan, J. Fluid Mech. **67**, 155 (1975).
[14] H. A. Rose and P. L. Sulem, J. de Physique **39**, 441 (1978).
[15] S.A.Orszag and G.S.Patterson, Phys. Rev. Lett. **28**, 76 (1972).
[16] M. Ottaviani and F. Porcelli, Proceedings of the 1994 EPS Conference, Montpellier.
[17] J. Wesson, private communication.

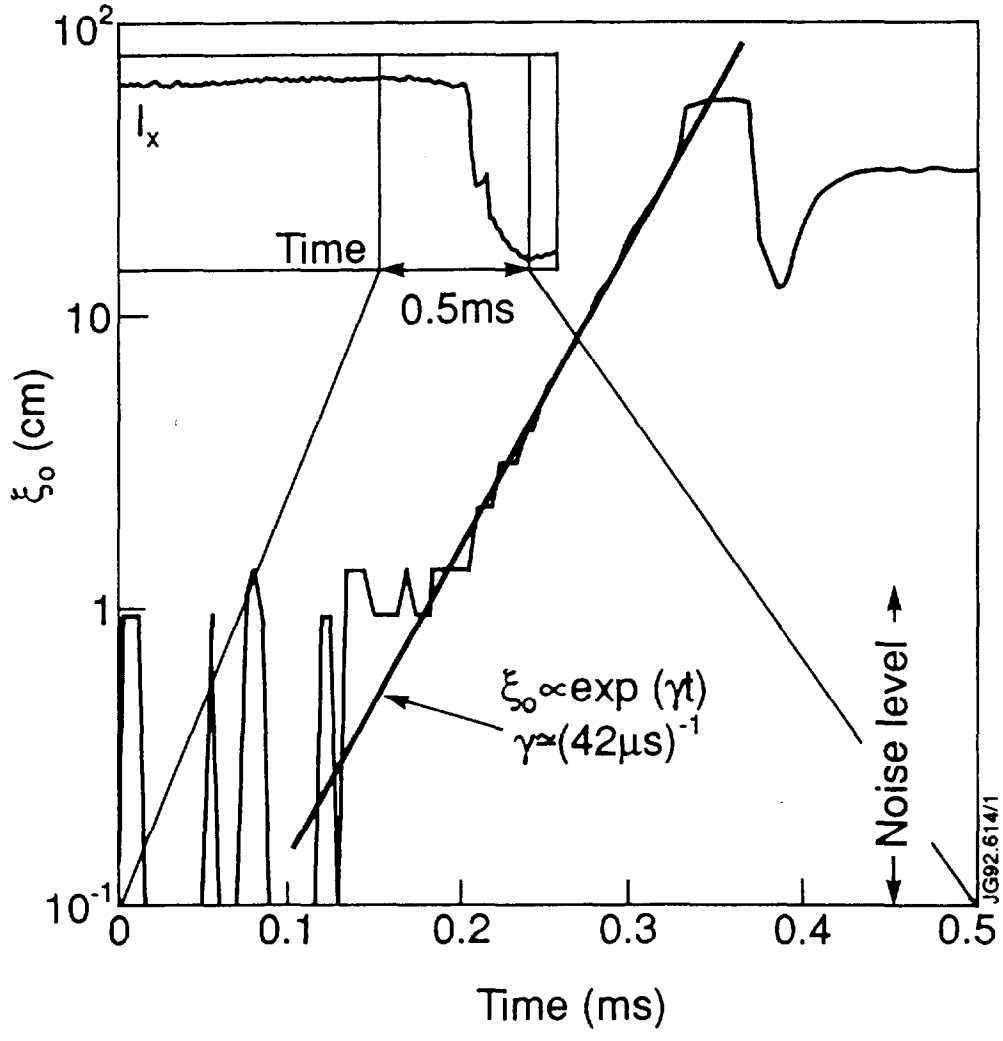

Fig.1. Evolution of the position of the peak of the soft X-ray emissivity during a fast sawtooth crash in JET.

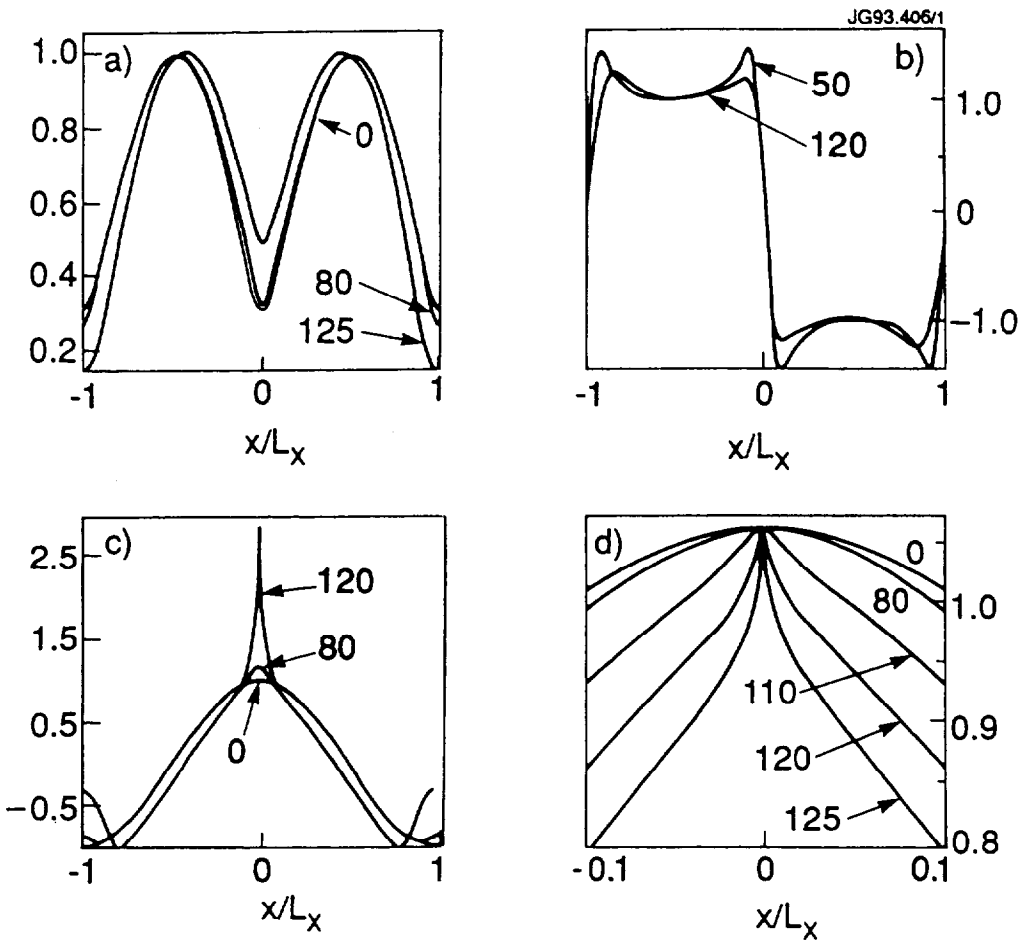

Fig. 2. Cross sections of a) $\delta\psi/(\delta\psi)_{x=L_x/2}$; b) $v_x/(v_x)_{x=-L_x/2}$; c) J; d) F versus x at $y=0$. The X-point is at $x=0$; the O-point of the second island chain is at $x=\pm L_x$. Times are indicated by the arrows.

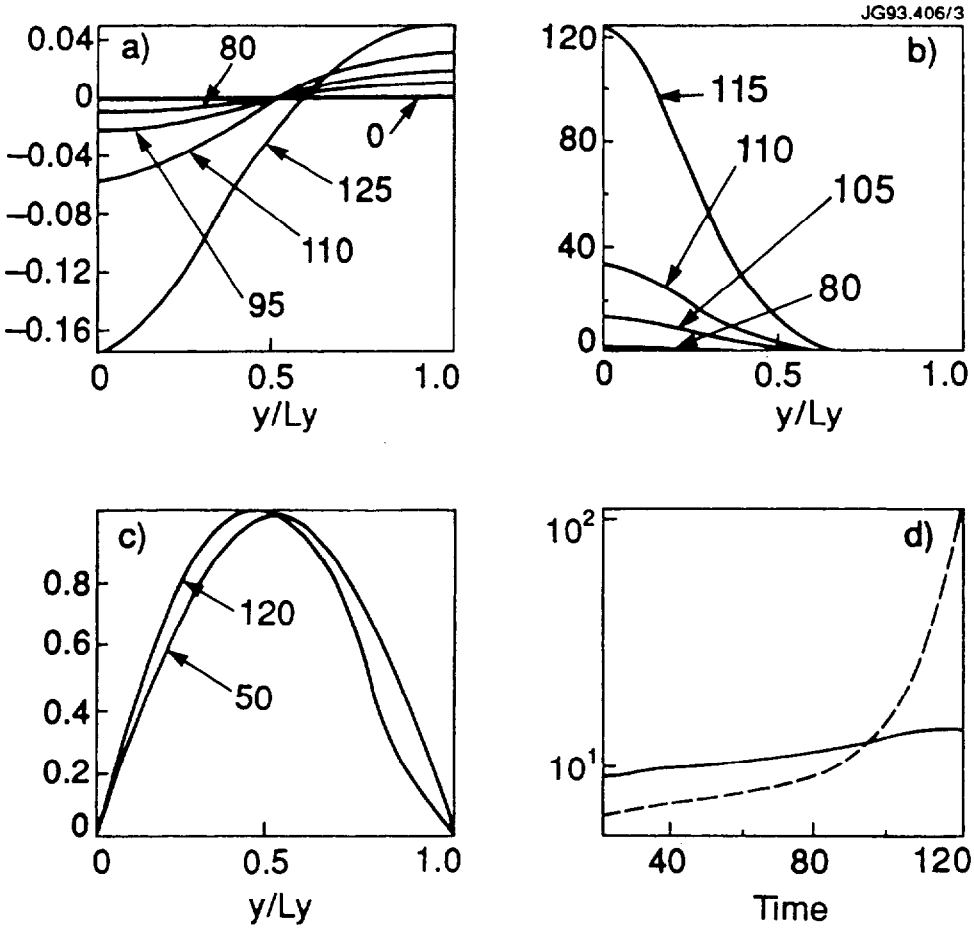

Fig. 3. Cross sections of a) $\delta\psi$; b) $\partial^2 F/\partial x^2$; c) $v_y/(v_y)_{y=L_y/2}$ versus y at $x=0$. The island's X- and O-points are at $y=0$ and $y=L_y$, respectively. Also, d) time dependence of the logarithm of the inverse scale lengths δ_φ^{-1} (solid line) and δ_J^{-1} (broken line).

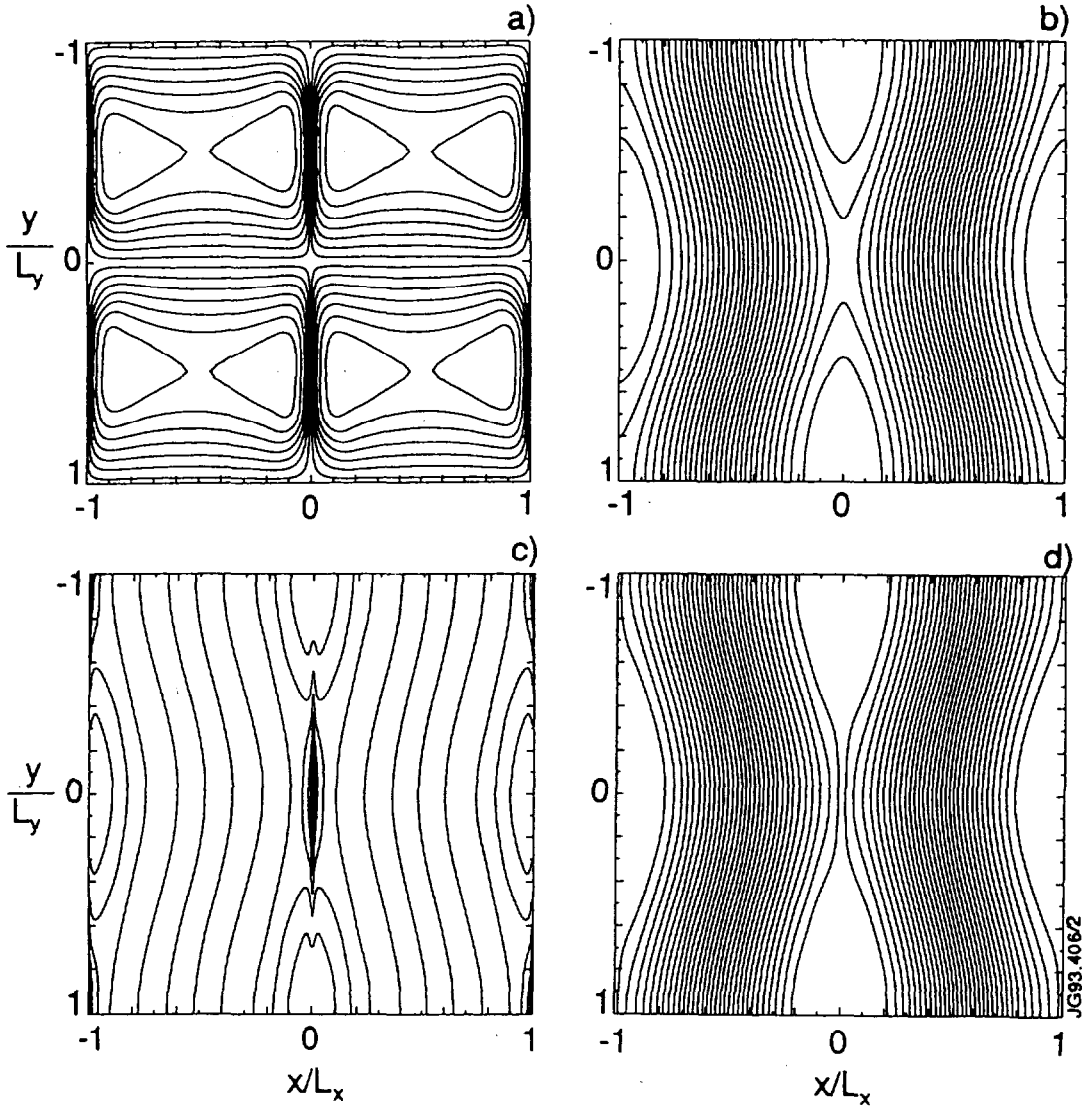

Fig. 4. Contour plots at $t=120$: a) φ; b) ψ; c) J; d) F.

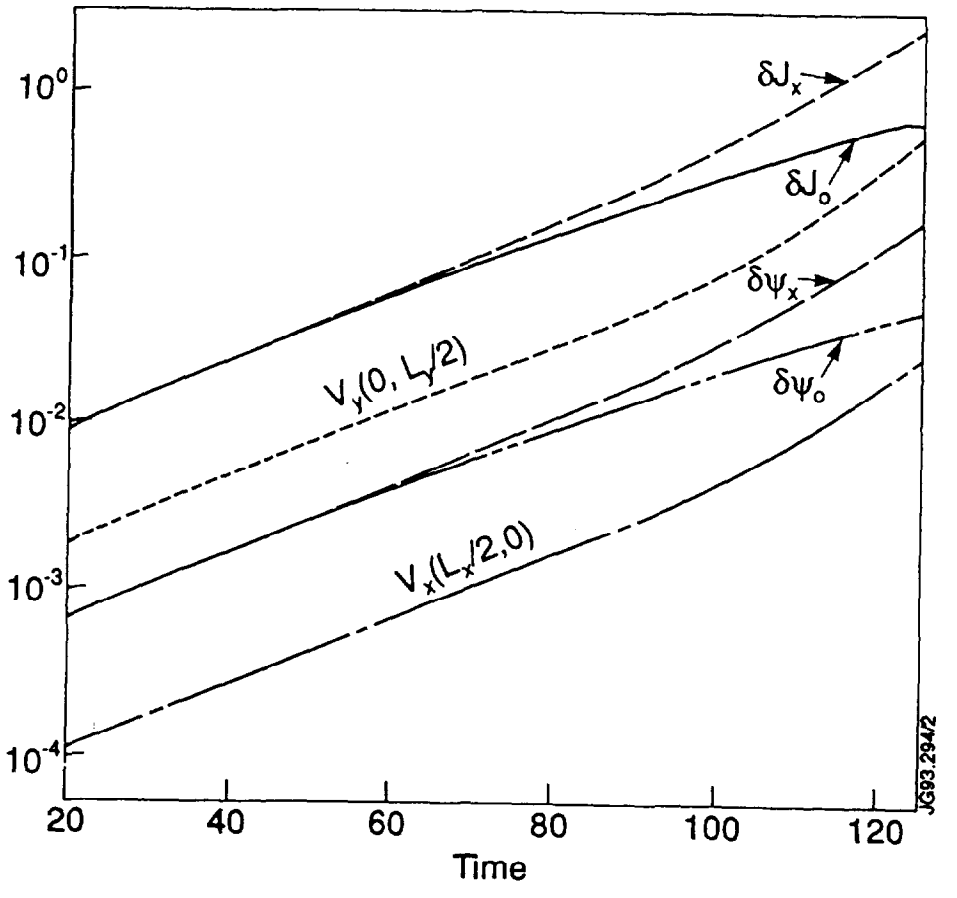

Fig. 5. Time dependence of $\delta\psi$ and δJ at the X- and O-points, of $v_x(-L_x/2,\ 0)$ and of $v_y(0,\ L_y/2)$.

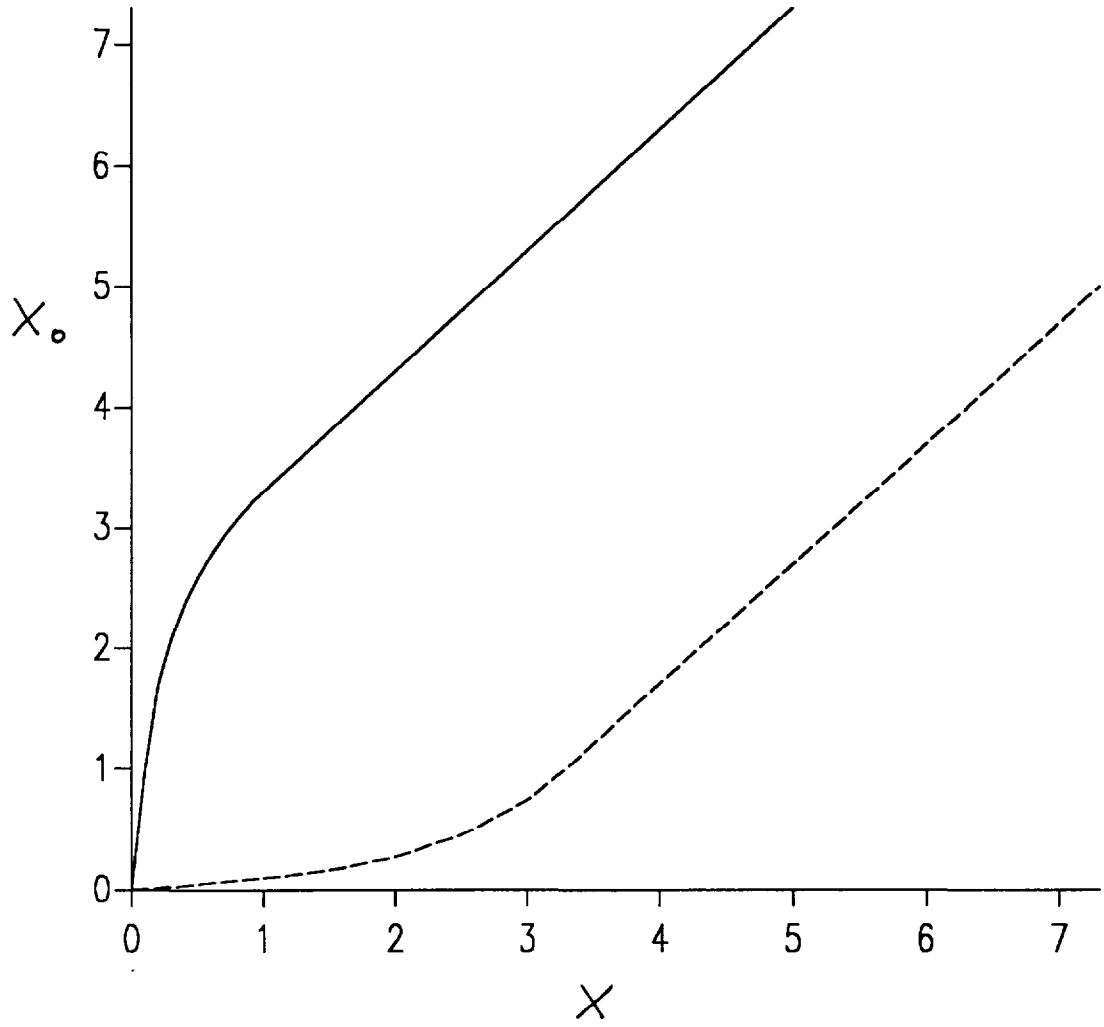

Fig. 6. Behaviour of x_o vs. x at the X-point (solid line) and at the O-point (broken line). $d = 1$ and $\delta = 0.1$ in this example.

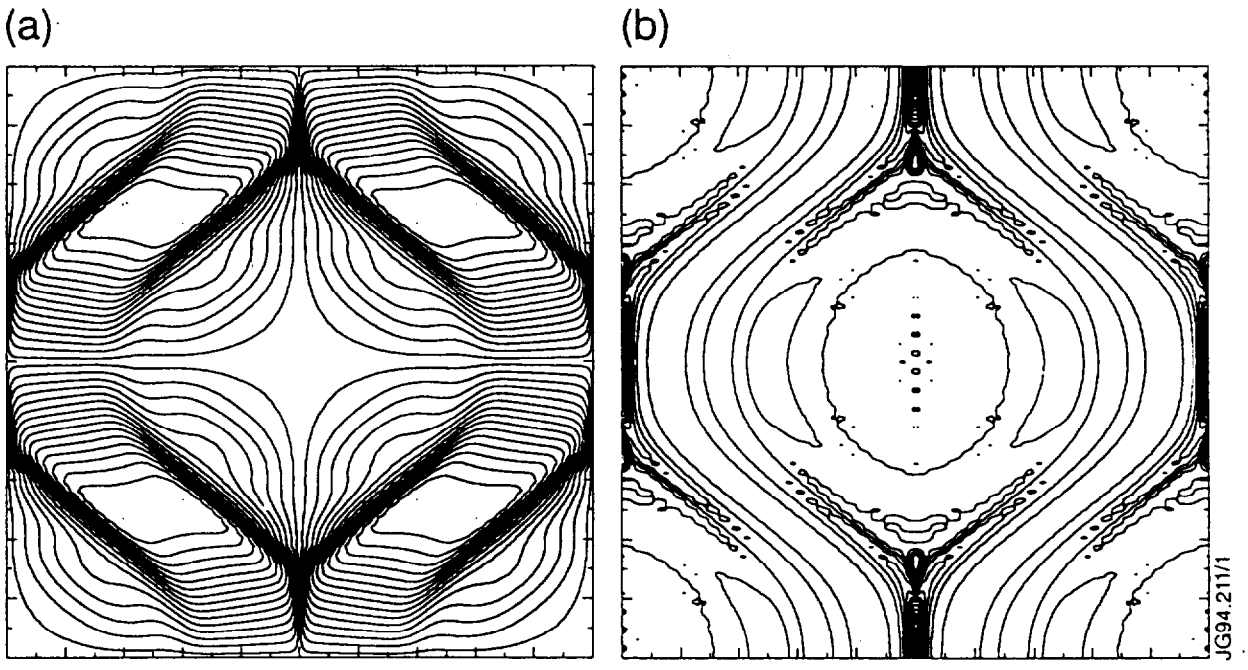

Fig. 7. Contour plots of a) the stream function φ and b) the current density J in the purely resistive case.